Available online at www.sciencedirect.com
SCIENCE DIRECT®
Global and Planetary Change 42 (2004) 167–176
GLOBAL AND PLANETARY CHANGE
www.elsevier.com/locate/gloplacha

Antarctic subglacial sedimentary layer thickness from receiver function analysis

S. Anandakrishnan*, J.P. Winberry

Department of Geosciences and EMS Environment Institute, The Pennsylvania State University, University Park, PA 16802, USA

Received 13 June 2003; received in revised form 14 October 2003; accepted 20 October 2003

Abstract

A large part of the West Antarctic Ice Sheet (WAIS) is on the West Antarctic rift system. The base of the ice sheet is currently below sea level, which has lead some researchers to suggest that its size, volume, and flow characteristics are particularly sensitive to climate change. Much of the ice is transported from the interior to the coast via fast-flowing glaciers and ice streams whose flow dynamics are strongly controlled by conditions at the bed. Variations in basal temperature, water content, and the distribution and lithology of sedimentary basins and crystalline basement contribute to the complexity of the observed flow environments in West Antarctica. Determining those parameters will contribute to an improved ability to model the ice sheet accurately. We report on the characteristics of sedimentary layers beneath the Antarctic using broadband seismic techniques and their association with flow of the ice sheet.

Keywords: Antarctica; Receiver functions; Sedimentary layers; Ice streams

1. Introduction

Most of Antarctica is ice covered. It is becoming increasingly clear that the flow of the ice is related to subglacial parameters such as heat flow, water distribution, basal roughness, and variations in geology. In particular, a better mapping of the distribution and characteristics of sedimentary basins is needed to fully model the flow of ice streams that drain much of the interior of the West Antarctic. Potential field methods (gravity and magnetics) can help to constrain the distribution of sedimentary and igneous provinces, but these methods are inherently nonunique and are generally low resolution. At the other extreme, reflection- and refraction-seismic techniques are accurate, have high resolution, and can uniquely identify the seismic velocities of subglacial units (which are related to the mechanical and hydrological properties of the sediments). This technique, particularly when allied to spot drilling to calibrate the results, is expensive, slow, and logistically intensive to conduct over wide areas.

A solution with intermediate resolution, low cost, and low logistics impact is to use naturally occurring seismic activity (in general, off-continent earthquakes because of the paucity of intracontinental seismic activity) recorded on broadband seismometers in-

* Corresponding author. Tel.: +1-814-863-6742; fax: +1-814-863-8724.
E-mail address: sak@essc.psu.edu (S. Anandakrishnan).

0921-8181/$ - see front matter © 2004 Elsevier B.V. All rights reserved.
doi:10.1016/j.gloplacha.2003.10.005

stalled at the surface of the ice sheet. The seismic energy travels through the mantle, crust, upper crust, and ice, and is modified at each of these interfaces if there is a significant acoustic impedance contrast (acoustic impedance is the product of seismic velocity and density). In this paper, we demonstrate that this technique can be used to identify sedimentary units beneath the ice sheet.

2. Receiver function technique

The one-dimensional seismic velocity structure beneath a broadband seismic recording station can be determined by the method of receiver functions (see Langston, 1977, 1979; Ammon et al., 1990; Ammon, 1991). The method assumes that the direct compressional wave arrival (Ṕ, which is generally the first arriving energy at teleseismic distances) will dominate the vertical component of a three-component seismograph station. By contrast, the radial (horizontal) component will be dominated by any compressional-to-shear wave converted waves (ṔṠ), which are produced by seismic velocity contrasts between geologically significant layers present beneath the stations. The amplitude of the ṔṠ converted wave is proportional to the magnitude of the acoustic impedance contrasts between these layers.

In the case of a relatively massive low-velocity (or low-acoustic impedance) layer at the surface, there is significant reverberation within that column. The acoustic impedance of glacier ice is $Z=\rho\times\upsilon_p=3.54\times10^6$ kg m^{-2} s^{-1}, which is substantially lower than the acoustic impedance for crystalline basement rocks, but is comparable to some sedimentary rocks ($\upsilon_p\approx2$–2.5 km s^{-1} and $\rho\approx2$ kg m^{-3}) (Sheriff and Geldart, 1995). We investigate two simple end-members of (a) two layers (ice over crystalline basement) or (b) three layers (ice over sediments over basement) for the structure beneath the ice sheet. As we will demonstrate, broadband seismic methods in Antarctica (and Greenland) will be unlikely to resolve fine structure at depth as is routinely done with continental (nonice sheet) seismic stations. The ice sheet reverberation introduces spectral peaks at frequencies n/T, $n=1,\ldots$, where T is the two-way travel time through the ice sheet. For a 2-km-thick ice sheet, the reverberations at approximately 0.5, 0.7, 1 Hz, and their multiples (1.4, 1.5, 2,... Hz) dominate the spectrum of the data. The reflection coefficient at the surface is $R=-1$, a perfect reflector, and at the bed is $R=0.6$ (for crystalline basement rocks, assuming $\upsilon_p=5.7$ km s^{-1}, and density $\rho=2.5$ kg m^{-3}). Attenuation in ice is relatively low at these frequencies (Bentley and Kohnen, 1976), resulting in little diminution in the amplitude of the reflections. The signal is reduced to 10% of its initial amplitude after four reverberations, during which time (up to 10 s) much of the upper crustal structure is masked.

In Fig. 1, we demonstrate the effects of adding a 2-km ice sheet to a simple one layer earth model (note the difference in horizontal scale among the three panels). We have generated synthetic receiver functions demonstrating the effect of a 2-km-thick ice sheet and the effects of a 200-m-thick sedimentary layer directly beneath the ice. In panel (a), the receiver function is for a model with no ice sheet, but with a 30-km-thick crust (top curve). The ṔṠ conversion at the Mohorovičić discontinuity (abbreviated Moho hereafter) is apparent at approximately 5 s, as are the Moho multiples at 15 s. The addition of a 2-km-thick ice sheet obscures all the data up to the Moho multiples (second curve, labeled "30 km with ice"). The third curve is for a model of ice sitting directly on a half space (labeled "ice over half space") demonstrating that much of the energy in the first 10 s of the receiver function is from the ice alone. Finally, the bottom curve is a receiver function of data from station BYRD.

In panel (b) we concentrate on the first 2 s of the receiver function to show the effects of ice (top curve) and ice over sediments (bottom curve). The receiver functions show the direct arrival (P), and the converted wave at the base of the ice (Ps), and the multiple off the base of the ice (Ppms). Addition of a 200-m-thick low-velocity sediment layer ($\upsilon_p=2.4$ km s^{-1}, $\rho=2$ kg m^{-3}) tends to shift the Ps and multiple arrivals by the transit time of that layer. No additional arrival from the interface between the ice and the sediments is generated, because of the low acoustic impedance contrast between them. In panel (c), the synthetic data presented in panel (a) were low pass filtered at 0.2 Hz, to demonstrate that the direct Ps is not visible, but that the Moho multiple can be seen.

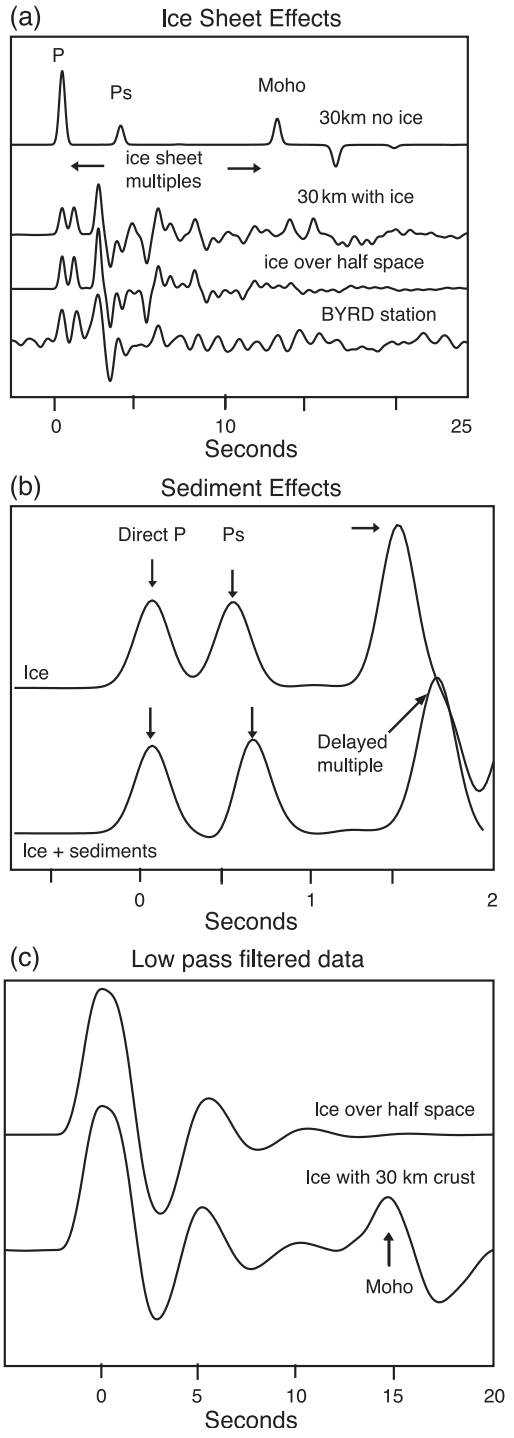

3. Data analysis

3.1. Data collection

We deployed seismic stations in Antarctica as part of the Anubis project (Anandakrishnan et al., 2000) to expand the data available for Antarctica (Fig. 2). Our work was concentrated in West Antarctica; the inset panel is a map of the whole continent, showing the stations of the Global Seismic Network as well as two stations in East Antarctica from the Tamseis experiment. The continent is more than 98% ice covered, and there are only two permanent manned bases on the ice sheet, thus limiting the use of traditional station-based seismic data collection. We developed new systems to reliably work over the winter months (Anandakrishnan, 1999) so that we could answer questions about local seismicity and earth structure that are difficult or impossible to do from stations at the perimeter of the continent or off the continent. The seismometers (Guralp Systems CMG3-ESP) were installed in 2-m-deep pits to reduce wind noise, reduce the temperature variations, as well as to improve coupling. The stations were placed 100 m from any surface structures (solar panels and wind generators) to reduce noise. The data were stored locally and retrieved once a year. In Table 1, we summarize the data collected and our results. We only used events greater than magnitude $M = 6.0$, and within the range of offsets $\Delta = 40-85°$. The paucity of events in that offset range is reflected in the small number of events analyzed; most of the events were subduction zone events from the Kermadec Trench or from west coast of S America.

Local seismicity has been hypothesized to be low (Adams and Akato, 1986; Johnston et al., 1994; Johnston, 1987), but our deployment found that there were many small events that were not being recorded by the global network (Winberry and Anandakrishnan, 2003). Surface wave dispersion measurements can give an image of the deep structure of the continent and areally averaged images of the crust

Fig. 1. (a) Synthetic receiver functions for a one-layer crust model, two-layer model (ice over crust), and a one-layer ice over half-space model, as well as data from station BYRD. (b) The first 2 s of the receiver function for the case of ice over basement and ice plus sediments over basement. (c) Low pass filtered versions of the synthetics, showing the Moho multiple.

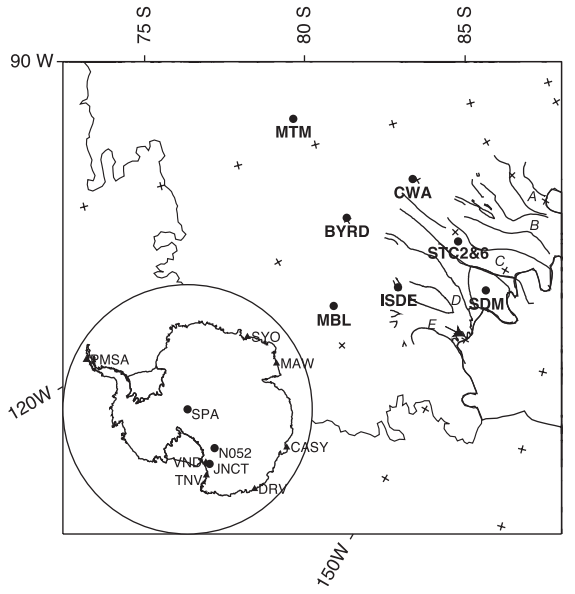

Fig. 2. Map showing the stations used in this analysis. In addition, we have outlined the ice streams of the Siple Coast and labeled ice stream A–E (flow is from east to west). We have also marked the Global Seismic Network (GSN) stations with triangles.

(Roult et al., 1994; Roult and Rouland, 1994; Ritzwoller et al., 2001), but are not capable of resolving basin-scale sedimentary structures (and even smaller scale horst-and-graben structure) that are likely to be important for ice sheet and ice stream flow. Here we report on the sedimentary basin imaging.

3.2. Receiver function minimization

We use a simple grid search technique where we fixed the Poisson's ratio in the layers and vary shear wave velocity υ_s and layer thickness L to minimize the error between modeled and recorded receiver functions. We used a frequency domain deconvolution of the vertical and radial components, with water level stabilization and a Gaussian filter (e.g., Clayton and Wiggins, 1976; Ammon, 1991), to compute the receiver functions.

The synthetic seismograms were computed using the method of Randall (1989), which is based on the reflection matrix technique (Kennett, 1983). The synthetics were then deconvolved using the same parameters (water level and filter width) as were used with the data. We calculate the L_1 norm of the error, $L_1 = |h(t)\text{-}h_s(t)|$, where $h(t)$ is the receiver function and $h_s(t)$ is the synthetic receiver function. The location of the minimum $(\upsilon_s,L)_{min}$ in the L_1 map is the best fit of our model to the data. In all cases, for the synthetic seismograms, we included an ice layer of known thickness determined by seismic reflection sounding at stations CWA and STC (Anandakrishnan et al., 1998; Atre and Bentley, 1993, respectively), radio echo sounding at stations BYRD, MBL, ISDE, and MTM (Rose, 1979; Drewry, 1983). In addition, coring to bedrock near SDM (Siple Dome core) and BYRD (Gow, 1970) reveal the ice thickness at those locations. The error in the ice thickness is 30 m for SDM, BYRD, STC, and CWA, and is greater at ISDE and MBL, where the ice thickness is interpolated from the relatively coarse grid of flight lines (Drewry, 1983). Stations MBL and ISDE are near an oversnow seismic traverse with quoted accuracy of 40 m (Bentley and Chang, 1971) as well as a dense radio echo sounding grid (Bindschadler et al., 1996) with an accuracy of 5 m, so we can extrapolate somewhat between them and estimate an error of 50 m. The station with the poorest ice thickness determination is MTM, which is within the coarse radio echo sounding grid of Drewry (1983), but not on one of the lines. We estimate that the ice thickness error for MTM is 150 m.

The angle of incidence for the P and Ps arrivals at the base of the ice sheet is near vertical (the largest is 15° from the vertical). Thus, the piercing point of the seismic ray could be offset from the station location by as much as a kilometer for stations on 3-km-thick ice. For much of the region, subglacial topography is

Table 1
Table summarizing our measurements of sediment thickness

Station	Latitude	Longitude	Layer thickness		
			Ice (km)	Sediment (m)	Events
BYRD	S80°00.0′	W119°32.80′	2.26 ± 0.03	0 ± 50	4
ISDE	S80°00.0′	W134°59.61′	1.20 ± 0.05	0 ± 80	4
MBL	S78°05.58′	W130°13.45′	1.85 ± 0.05	260 ± 80	3
MTM	S79°29.76′	W100°00.74′	3.2 ± 0.15	550 ± 250	2
SDM	S81°36.89′	W148°51.00′	1.02 ± 0.03	300 ± 50	2
OND	S80°44.74′	W125°44.15′	2.25 ± 0.03	250 ± 50	2
STC2	S82°21.45′	W136°24.37′	1.05 ± 0.03	0 ± 50	2
STC6	S82°27.05′	W136°25.40′	1.00 ± 0.03	180 ± 50	2
N052	S79°32.64′	E145°44.93′	2.40 ± 0.03	300 ± 50	2
JNCT	S76°55.72′	E157°54.07′	0.80 ± 0.03	0 ± 50	2
SPA	S90°0′	E0°0′	2.80 ± 0.03	200 ± 50	2

subdued and the ice thickness changes little over a kilometer. However, the walls of the Bentley Subglacial Trench could be relatively steep (as much as 5°), contributing additional error to the ice thickness used at MTM, leading us to estimate a 150-m uncertainty for the ice thickness at MTM. Because of the uncertainty in subglacial topography surrounding the stations, we estimate a minimum ice thickness uncertainty of 30 m for all the data, with some sites having slightly higher uncertainties (Table 1). Note that in the work that follows, the ice thickness estimates impact the sediment thickness calculations, but not determinations of depth to Moho (we are working on Moho depth calculations but do not present those data here). A subglacial sediment layer thickness of 50 m would introduce a 70 ms delay in the multiple (relative to a model without sediments, and assuming $\upsilon_s = 1.1$ km s^{-1}, which is in midrange of our sediment velocities). This delay is the smallest that we can resolve with our data sampled at an interval of 25 ms.

3.3. Sediment layer thickness

The presence of a low-velocity sedimentary layer ($\upsilon_p = 2–2.5$ km s^{-1}, suggesting unlithified sediments) has been hypothesized to be a necessary but not sufficient condition for the fast flow of ice streams (Anandakrishnan et al., 1998). Subglacial sediments are a potential source region for a basal till layer that has been hypothesized as necessary for the fast flow of ice streams (Alley et al., 1986), or at least for the initiation of fast flow (Blankenship et al., 2001). Thus, mapping of sedimentary basins is needed to establish a region where ice streams could form and establish themselves, and regions where they are unlikely to do so. Two important variables for ice sheet modeling are the basal slip condition and the basal heat flow. The former of these is related to the presence of sediments (to generate till), and high heat flow (to generate basal meltwater); the latter is related to crustal thickness and mantle temperatures (which we do not treat in this paper).

We determine subglacial sedimentary layer thicknesses by exploiting the mismatch between the receiver function synthetics (for which we know the ice thickness independently from radio echo sounding or seismic reflection imaging) and the data. The Ps arrival from the base of the ice sheet will be absent if there is a well-matched subglacial layer beneath the ice. If the acoustic impedance of the ice and the sediments are similar (acoustic impedance $Z = \upsilon_p \times \rho$, the product of seismic velocity and density) then that boundary will be relatively transparent to the seismic waves. Thus, the Ps arrival in the data will be from the base of sediments. We can fix the ice thickness, and perform a grid search over a range of sediment thickness L, and shear wave velocity υ_s (we assume a fixed Poisson's ratio $\nu = 0.25$, typical of WAIS sediments and Ross Sea sediments (Rooney et al., 1987b) and do not independently calculate the compressional wave velocity υ_p). The location of the minimum error corresponds to the best fit for subglacial sedimentary layer thickness and velocity. The upper bound for the shear wave velocity in the sediments is $\upsilon_s = 1.5$ km s^{-1}; for higher velocities, there would be separate arrivals from both the ice/sediment interface as well as the sediment/rock interface. The results are robust with respect to changes in processing parameters such as water level and choice of filter.

The data are summarized in Fig. 3 (West Antarctic sites) and Fig. 4 (East Antarctic sites). The data effectively group into two categories: no-sediment sites (BYRD, ISDE, STC2, JNCT in East Antarctica), and sites with 200–300 m of sediments (the rest of the stations except for MTM). Once again, MTM, in the heart of the Bentley Subglacial Trench has substantially different subglacial characteristics, with a sediment layer thickness twice that of the other stations. Thick packets of low-velocity sediments have been imaged beneath ice stream B (1 km of low-velocity sediments was measured at UPB, 83.5°S, 138°W) (Rooney et al., 1987a,b) and ice stream C (2 km of sediments was estimated from refraction sounding at Ridge BC: 82°28′ S 136°W) (Munson and Bentley, 1992).

As sediments are necessary for fast flow, we first examine the sites without sediments. We make the distinction between "slow flow" where the surface speed can be completely explained by internal deformation within the ice, and "fast flow" where there must be a component of basal sliding (either sliding over a water layer, plastically deforming a subglacial till layer, or deforming a meter-thick till layer; see Paterson (1994) for review). The association between fast flow and sediments applies to the latter two sliding mechanisms, as both require a source of

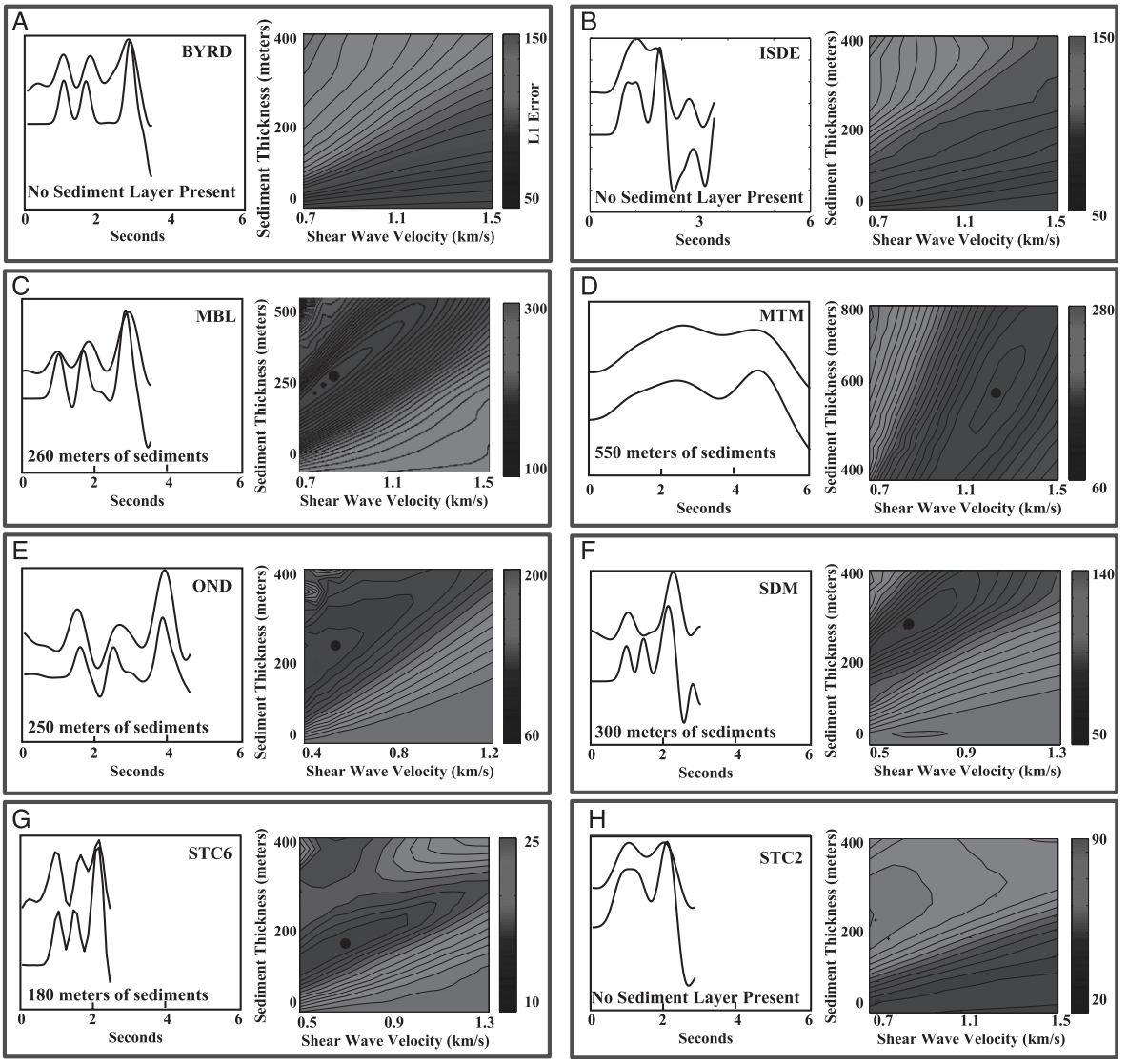

Fig. 3. Sediment layer thickness in West Antarctica. Each panel has the receiver functions in the left panel (synthetic above the data), and the L_1 error between the synthetic and the data in the right panel. When a significant minimum is present, we have marked it with a circle.

erodible sediments to supply the subglacial layer as the till material is transported to the coasts. All these locations are slow flowing, including STC2, which is on a distinct, slow-flowing "island" of ice surrounded by faster-flowing ice. The streamlines around the island are apparent in satellite imagery (Fig. 5) and in measured velocity vectors (Whillans and van der Veen, 1993; Hodge and Doppelhammer, 1996; Anandakrishnan and Alley, 1997) in the middle of ice stream C. The nearby station STC6 is 7 km away, but is underlain by 180 m of low-velocity sediments and is faster flowing than STC2 (although they have similar ice thicknesses, driving stresses, and we assume that heat flow is not substantially different over that small a region). Thus, we suggest that the only major distinction between the sites is the difference in subglacial sediments, which is sufficient to explain the island of stagnant ice inside ice stream C.

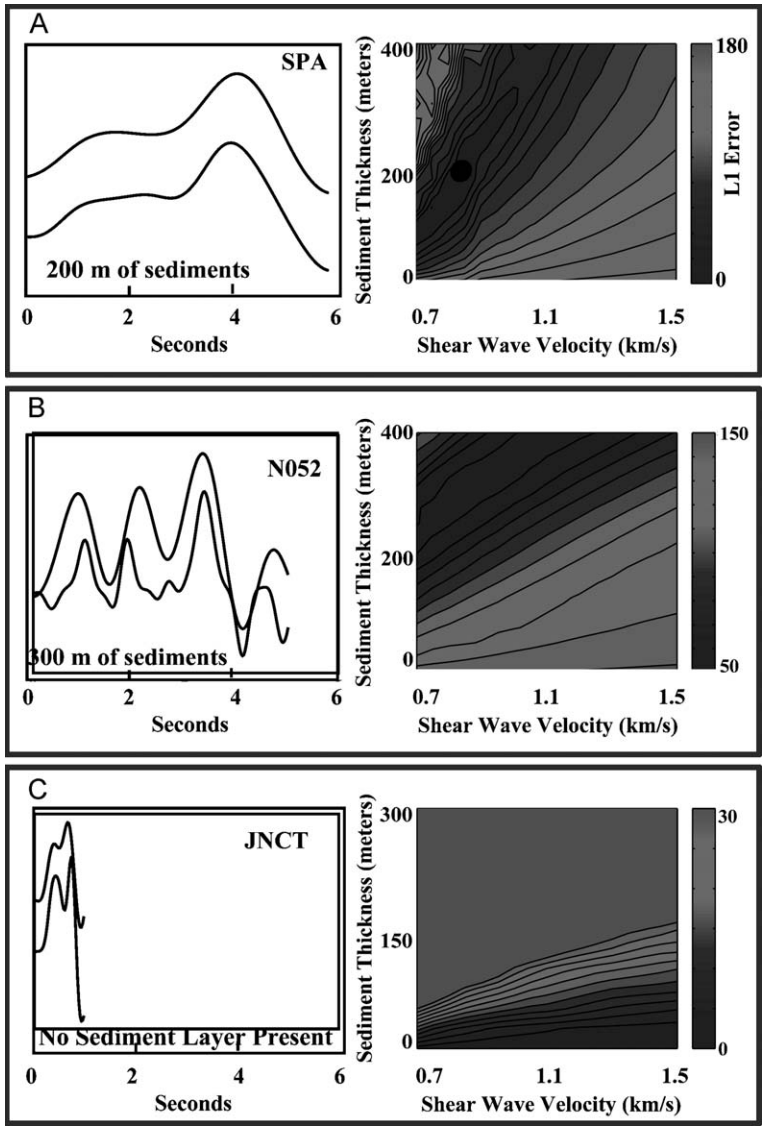

Fig. 4. Sediment layer thickness determination. Plots are similar to Fig. 3.

Station ISDE is on the slow-flowing interstream ridge between ice streams D and E. Ice thickness and driving stress are not dramatically different between ISDE and the on-stream ice; nevertheless, there is a significant difference in flow speed. We suggest that the absence of sediments beneath ISDE is the cause for the location of the interstream ridge and that the ice streams would not be able to migrate laterally across the ridge. Similarly, BYRD station is near the onset of streaming flow of ice stream D, but the tributary of fast-flowing ice that feeds ice stream D passes to south and north of BYRD; we suggest that they do so because of the absence of sediments at BYRD. Significantly, station OND (on ice stream D, and near the onset of fast flow) does have a thick packet of sediments.

Stations OND, STC6, and MBL all have significant thicknesses of sediment and all are associated with fast-flowing ice. We have no measurement of the flow velocity of MTM. Finally, station SDM, on Siple

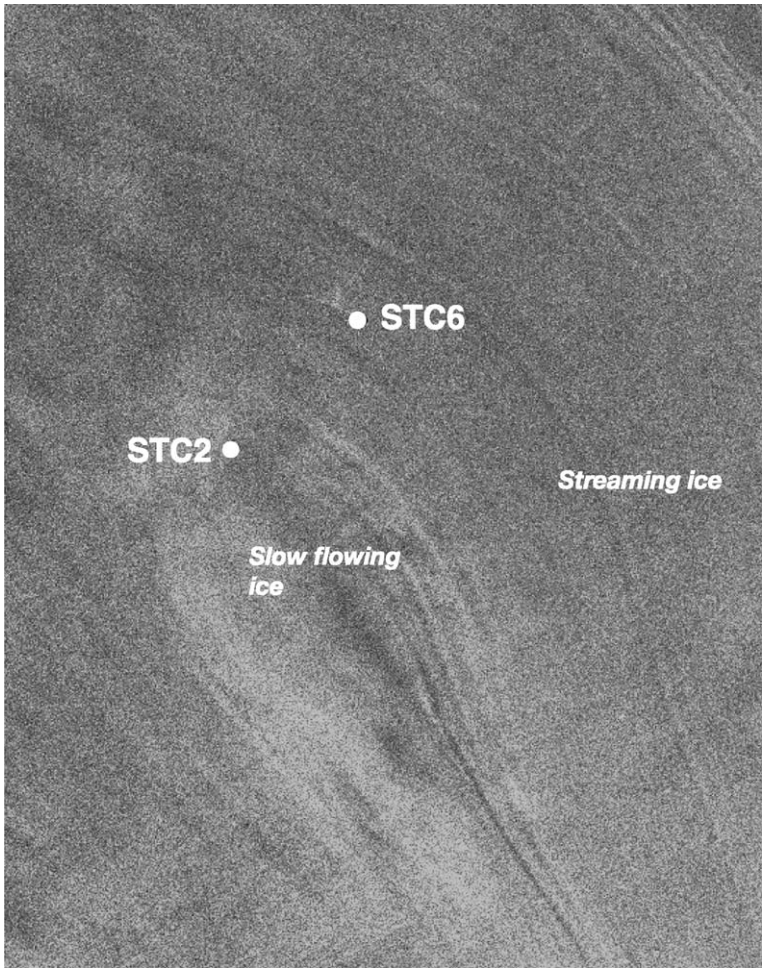

Fig. 5. Radarsat imagery of ice stream C (25-m resolution), showing the slow-flowing island in the middle, and the streamline associated with the faster-flowing stream. Stations STC2 and STC6 are marked with circles.

Dome, has thick sediments underlying the ice, but is slow flowing. This dome of ice has been hypothesized to be long-lived and persistent through the last glacial–interglacial cycle (Conway et al., 1999). As we have emphasized, the presence of sediments is not sufficient to initiate fast flow. This is likely to be particularly true in regions of thinner ice (SDM has 1020 m of ice, compared to an average of 2000 m in the interior of the ice sheet where the ice streams initiate.

In East Antarctica (Fig. 4), we measured no sediments at JNCT, but found 300 m of sediments at N052. This is significant because station N052 is in the middle of the Wilkes Subglacial Basin, which would be a low-lying (partially water-covered) basin if the East Antarctic Ice Sheet were removed. The presence and age of sediments in this basin are relevant to the history, dynamics, and age of the EAIS. Work in progress will map the sediment thickness in greater detail across the Wilkes Basin. Finally, station SPA at S. Pole also revealed the presence of a thick layer of sediments. Suggestions of a ‘‘fossil’’ subglacial lake (a lake that has since frozen) (Price et al., 2002) would be consistent with the presence of sediments. We do not make associations between flow and sediments in East Antarctica because over most of this ice sheet, the ice flows by internal deformation, with ice streaming limited to a few regions around the

coast. The presence or absence of sediments in E Antarctica is more likely to be useful for stratigraphic interpretations of age and history.

4. Conclusion

We have demonstrated that the receiver function technique suffers from some limitations when used for data collected on ice sheets. However, that limitation applies primarily to the layering within the upper crust. The technique can be used to get high-resolution upper crustal information for the presence or absence of a sedimentary layer directly beneath the ice. If the ice thickness is known by independent means (radio echo sounding or seismic reflection), then the mismatch between the Ps arrival from the base of the ice in the synthetic seismogram and the Ps arrival in the data can be used to determine the properties of that layer. We have used that method to show that there is a good (but not perfect) association between the absence of sediments and slow flow, and the presence of sediments and fast flow. This technique is relatively efficient to implement in the field, only requiring a single seismometer. It can be used to better constrain aerogeophysical data sets and satellite gravity data.

Acknowledgements

We thank J. Bowling, P.G. Burkett, R.C. Henry, B.R. Long for field assistance. We thank D.E. Voigt for invaluable support during the planning and deployment of this experiment. We thank Raytheon Polar Services, Kenn Borek Air, and the NY Air National Guard for their support. This work was support by the National Science Foundation (grants 9615147 and 9996272).

References

Adams, R.D., Akato, A.M., 1986. Earthquakes in continental Antarctica. J. Geodyn. 6, 263–270.

Alley, R.B., Blankenship, D.D., Bentley, C.R., Rooney, S.T., 1986. Deformation of till beneath ice stream B, West Antarctica. Nature 322, 57–59.

Ammon, C.J., 1991. The isolation of receiver effects from teleseismic P waveforms. Bull. Seismol. Soc. Am. 81, 2504–2510.

Ammon, C.J., Randall, G.E., Zandt, G., 1990. On the nonuniqueness of receiver function inversions. J. Geophys. Res. 95, 15303–15318.

Anandakrishnan, S., 1999. Penguins everywhere: GNU/Linux in Antarctica. IEEE Softw. 16, 90–98.

Anandakrishnan, S., Alley, R.B., 1997. Stagnation of ice stream C, West Antarctica by water piracy. Geophys. Res. Lett. 24, 265–268.

Anandakrishnan, S., Blankenship, D.D., Alley, R.B., Stoffa, P.L., 1998. Influence of subglacial geology on the position of a West Antarctica ice stream from seismic measurements. Nature 394, 62–65.

Anandakrishnan, S., Voigt, D.E., Burkett, P., Long, B., Henry, R.C., 2000. Deployment of a broadband seismic network in West Antarctica. Geophys. Res. Lett. 27, 2053–2056.

Atre, S.R., Bentley, C.R., 1993. Laterally varying basal conditions under ice streams B and C, West Antarctica. J. Glaciol. 39, 507–514.

Bentley, C.R., Chang, F., 1971. Geophysical exploration in Marie Byrd Land, Antarctica. In: Crary, A.P. (Ed.), Antarctic Snow and Ice Studies, II. Antarctic Research Series, vol. 16. AGU, Washington, DC, pp. 1–38.

Bentley, C.R., Kohnen, H., 1976. Seismic refraction measurements of internal friction in Antarctic ice. J. Geophys. Res. 81, 1519–1526.

Bindschadler, R.A., Vornberger, P.L., Blankenship, D.D., Scambos, T.A., Jacobel, R., 1996. Surface velocity and mass balance of ice stream D and E, West Antarctica. J. Glaciol. 42, 461–472.

Blankenship, D.D., et al., 2001. Geologic controls on the initiation of rapid basal motion for West Antarctic ice streams: a geophysical perspective including new airborne radar sounding and laser altimetry results. In: Alley, R.B., Bindschadler, R.A. (Eds.), The West Antarctic Ice Sheet: Behavior and Environment. Antarctic Research Series, vol. 77. AGU, Washington, DC, pp. 283–296.

Clayton, R.J., Wiggins, R.A., 1976. Source shape estimation and deconvolution of teleseismic body waves. Geophys. J. R. Astron. Soc. 47, 151–177.

Conway, H., Hall, B.L., Denton, G.H., 1999. Past and future grounding-line retreat of the West Antarctic Ice Sheet. Science 286, 280–283.

Drewry, D.J. (Ed.), 1983. Antarctica: Glaciological and Geophysical Folio, vol. 2. Scott Polar Research Institute, Cambridge Sheet 4.

Gow, A.J., 1970. Preliminary results of studies of ice cores from the 2164 m deep drill hole, Byrd Station, Antarctica. IASH 86, 78–90.

Hodge, S.M., Doppelhammer, S.K., 1996. Satellite imagery of the onset of streaming flow of ice streams C and D, West Antarctica. J. Geophys. Res. 101, 6669–6677.

Johnston, A.C., 1987. Suppression of earthquakes by large continental ice sheets. Nature 330, 467–469.

Johnston, A.C., Coppersmith, K.J., Kanter, L.R., Cornell, C.A., 1994. The earthquakes of stable continental regions. Assesment

of large earthquake potential, vol. 1. Tech. rep. Electric Power Research Institute, Palo Alto.

Kennett, B.L.N., 1983. Seismic Wave Propagation in Stratified Media. Cambridge Univ. Press, Cambridge.

Langston, C.A., 1977. The effect of planar dipping structure on source and receiver responses for constant ray parameter. Bull. Seismol. Soc. Am. 67, 1029–1050.

Langston, C.A., 1979. Structure under Mount Rainier, Washington, inferred from teleseismic body waves. J. Geophys. Res. 84, 4749–4762.

Munson, C.G., Bentley, C.R., 1992. The crustal structure beneath ice stream C and ridge BC, West Antarctica from a seismic refraction and gravity pro-file. In: Yoshida, Y., Kaminuma, K., Shiraishi, K. (Eds.), Recent Progress in Antarctic Earth Science. TERRAPUB, Tokyo, Japan, pp. 507–514.

Paterson, W.S.B., 1994. The Physics of Glaciers, 3rd ed. Pergamon, Tarrytown, NY.

Price, P.B., et al., 2002. Temperature profile for glacial ice at South pole: implications for life in a nearby subglacial lake. Proc. Natl. Acad. Sci. 99, 7844–7847.

Randall, G.E., 1989. Efficient calculation of differential seismograms for lithospheric receiver functions. Geophys. J. Int. 99, 469–481.

Ritzwoller, M.H., Shapiro, N.M., Levshin, A.L., Leahy, G.M., 2001. The structure of the crust and upper mantle beneath Antarctica and the surrounding oceans. JGR 106, 30645–30670.

Rooney, S.T., Blankenship, D.D., Alley, R.B., Bentley, C.R., 1987a. Till beneath ice stream B: 2. Structure and continuity. J. Geophys. Res. 92, 8913–8920.

Rooney, S.T., Blankenship, D.D., Bentley, C.R., 1987b. Seismic refraction measurements of crustal structure in West Antarctica. In: McKenzie, G.D. (Ed.), Gondwana Six: Structure, Tectonics and Geophysics. Geophysical Monograph Series, vol. 40. American Geophysical Union, Washington, DC, pp. 1–7.

Rose, K., 1979. Characteristics of ice flow in Marie Byrd Land, Antarctica. J. Glaciol. 24, 63–74.

Roult, G., Rouland, D., 1994. Antarctica: I. Deep structure investigations inferred from seismology; a review. Phys. Earth Planet. Inter. 84, 15–32.

Roult, G., Rouland, D., Montagner, J.P., 1994. Antarctica: II. Upper-mantle structure from velocities and anisotropy. Phys. Earth Planet. Inter. 84, 33–57.

Sheriff, R.E., Geldart, L.P., 1995. Exploration Seismology, 2nd ed. Cambridge Univ. Press, Cambridge.

Whillans, I.M., van der Veen, C.J., 1993. New and improved determinations of velocity of ice streams B and C, West Antarctica. J. Glaciol. 39, 483–490.

Winberry, J.P., Anandakrishnan, S., 2003. Seismicity and neotectonics of West Antarctica. Geophys. Res. Lett. 30, 1932–1935 (doi:10.1029/2003GL017801).